Journal of Cluster Science
https://doi.org/10.1007/s10876-022-02395-3

ORIGINAL PAPER

Low Dose of Green Synthesized Silver Nanoparticles is Sufficient to Cause Strong Cytotoxicity via its Cytotoxic Efficiency and Modulatory Effects on the Expression of *PIK3CA* and *KRAS* Oncogenes, in Lung and Cervical Cancer Cells

Hanan A. Bin Saeed[1] · Maha H. Daghestani[1] · Khushboo Ambreen[2] · Mazin H. Daghestani[3] · Sabah A. Al-Zahrani[4] · Hussah Alobaid[1] · Nawal M. AL-Malahi[1]

Received: 26 June 2022 / Accepted: 15 November 2022

Abstract
The impressive role of silver nanoparticles (AgNPs) is well identified for cancer therapy. However, safety concerns have been raised about the adverse effects of high-doses of chemically-synthesized-AgNPs that release many hazardous residues and in turn diminish the anticancer property of AgNPs. Hence, to overcome these side effects and to maintain the anticancer effectiveness of AgNPs at relatively low-doses, the present study utilizes a natural antitumor product *Ferula asafoetida* (FA) in the preparation of green synthesis of AgNPs and further focuses on its cytotoxic effects, against Lung and Cervical cancer cells. The successful green-synthesis of FA-AgNPs was confirmed via UV–Vis-spectroscopy, TEM, DLS, FTIR and IR. Based on cytotoxicity assay, the average low (6.25 µl) and high (25 µl) doses of FA-AgNPs were observed to cause severe cytotoxic effects on studied cancer cells. Furthermore, our study was also directed to check any possible antitumorigenic-modulatory-effects of low and high doses of FA-AgNPs on the expression of four oncogenes (*PIK3CA*, *KRAS*, *EGFR* and *ERBB3*). In RT-qPCR analysis, the low and high doses of FA-AgNPs caused significant($p < 0.01$) downregulation effects on the expression of *PIK3CA* and *KRAS* oncogenes, in treated-cancer cells. This is the first-report on the role of FA-AgNPs that induce strong cytotoxicity with its low-doses.

Keywords Silver nanoparticles · *Ferula asafoetida* · Green synthesis · Low dose · Cytotoxicity · Oncogenes · Lung and cervical cancer

Introduction

Cancer is a serious life-threatening disease causing a huge burden of death worldwide, accounting for approximately 10 million deaths in 2020 [1]. Over the past two decades, lung and cervical cancers are the two most common cancers that have been known to cause continuous escalating load of morbidity and mortality [2, 3].

Despite the advances in various effective drugs and therapies, majority of the cancer patients suffer unsatisfactory and depressive results in terms of short survival rate [4]. Hence, cancer treatment still demands newer approach in the form of more effective therapeutic benefits.

In recent growing and demanding field of nanotechnology, the extensive use of many popular nanoparticles is gaining primary attention towards the development of more effective and less costly anticancer drugs [5]. Among these prevalent nanoparticles, the anticarcinogenic potential of silver nanoparticles (AgNPs) is well established in numerous in vivo and in vitro studies in favor of lung, cervical, breast and colon cancer cells etc. [6–8]. In addition, a great number of scientists have highlighted the biological role of AgNPs

✉ Khushboo Ambreen
khushboo4march@gmail.com

[1] Department of Zoology, College of Science, Centre for Scientific and Medical Female Colleges, King Saud University, Riyadh, Saudi Arabia

[2] Department of Biotechnology, Integral University, Lucknow 226026, India

[3] College of Medicine, Umm Al-Qura University, Mecca, Saudi Arabia

[4] Department of Biochemistry, College of Science, King Saud University, Riyadh, Saudi Arabia

Published online: 13 December 2022

in tremendous antibacterial, anti-inflammatory, antiviral, antioxidant, antiplatelet, antifungal and anti-angiogenesis activities [9, 10].

Despite the widespread medical application of AgNPs, many previous studies have raised concern about the high doses of chemically synthesized AgNPs in terms of many acute and chronic adverse effects on human health. It has been shown that the repeated high dose exposure of chemically derived AgNPs exert various damaging effects on healthy cells such as liver damage, immune system toxicity, skin toxicity, reproductive toxicity and brain related disorder etc. [11, 12].

In addition, most of the chemicals used in the synthesis of AgNPs, are identified to release many hazardous residues that in turn play a key role to diminish the superior anticancer quality of AgNPs [13].

Hence, with the purposes to overcome these adverse effects as well as to maintain the anticancer effectiveness of AgNPs, researchers are giving more devotion towards new prominent techniques, among which the green synthesis method using plant extract has achieved great clinical application. The green synthesis of AgNPs utilizes reduction method in which plant extract containing phenolic compounds are used as reducing agents to reduce silver ions into AgNPs [14].

Ferula asafoetida (FA) is one of the popular medicinal plant species, belongs to the umbelliferae family, and is commonly used as a flavoring agent all over the world. In the past few years, the features of FA are demonstrated to have multiple biological and pharmacological activities including hepatoprotective, antiobesity, antioxidant, antimicrobial, anticarcinogenic, chemopreventive, neuroprotective, anticonvulsant, anthelmintic and antispasmodic etc. [15–17]. However, the most prominent biological features of FA are recorded in the form of substantial antioxidant capacity that in turn encourages strong anticancer efficiency against multiple cancer cells and promotes protective effects in favor of healthy cells [18, 19].

Hence, keeping in view the role of FA as a safer, natural and strong anticarcinogenic agent, the green synthesis of AgNPs utilizing the plant extract of FA may be proved highly beneficial in maintaining the anticarcinogenic efficiency of synthesized AgNPs at relatively low doses, against lung and cervical cancer.

Like other cancers, the etiology of lung and cervical cancers are characterized through the involvement of various genetic factors. Multiple previous studies suggest the major role of over-activated PI3K/AKT (phosphatidylinositol 3-kinase/protein kinase B) pathway as a genetic factor for the development of oncogenic process of lung and cervical cancers [20, 21]. The four oncogenes *PIK3CA* (Phosphatidylinositol-4, 5-Bisphosphate 3-Kinase, catalytic subunit Alpha), *KRAS* (Kirsten Rat Sarcoma), *EGFR* (Epidermal Growth Factor Receptor) and *ERBB3* (Erb-B2 Receptor Tyrosine Kinase 3) are reported to play a crucial role in the overactivation of PI3K/AKT pathway. Moreover, in most cases of solid tumors, these four genes are proved for high rate of mutations in terms of its over expression [22–24].

Hence, with the aim to check the anticarcinogenic efficiency of synthesized FA-AgNPs at molecular level, the present study for the first time determines the expression of these four oncogenes (*PIK3CA*, *KRAS*, *EGFR* and *ERBB3*) in FA aqueous extract and FA-AgNPs treated lung and cervical cancer cells.

The present study initially fucus on the preparation of FA aqueous extract and green synthesized FA-AgNPs, and then utilizes UV–Vis spectroscopy, TEM, DLS, FTIR and IR techniques to characterise the nano crystalline nature of FA-AgNPs. In the next, our study find out cytotoxic effects of FA extract and FA-AgNPs at different increasing doses, against lung (A549) and cervical (HeLa) cancer cells. However, the primary aim of our present study is to check the cytotoxic efficiency of low dose of green synthesized FA-AgNPs against studied cancer cells, and further to compare with the high dose effects of FA-AgNPs.

Furthermore, to evaluate the possible modulatory effects of low and high doses of FA extract and FA-AgNPs on the expression of four crucial oncogenes (*PIK3CA*, *KRAS*, *EGFR* and *ERBB3*), the study also performs RT-qPCR. To the best of the authors knowledge, until now there is no previous study that primarily evaluates the low dose efficiency of FA mediated green synthesized AgNPs in terms of its cytotoxicity and genetic alteration effects against A549 and HeLa cancer cells.

Materials and Methods

Collection and Preparation of FA Gum Aqueous Extract

Fresh FA gum was purchased from a local market in the Riyadh region of Saudi Arabia. The gum was properly washed through tap and distilled water to remove unwanted dust materials. The cleaned gum was air dried and deposited in sealed plastic bags. The aqueous extract (10% w/v) was prepared by adding the gum to boiled distilled water and was soaked overnight at room temperature. The prepared extract solution was filtered, identified as FA aqueous extract and stored at 4 °C for further use [25].

Green Synthesis of AgNPs, Using FA Aqueous Extract

With the aim to prepare green synthesized AgNPs, 50 ml of 1 mM aqueous solution of silver nitrate ($AgNO_3$) was initially prepared. 5 ml of FA aqueous extract was added

into the 50 ml aqueous solution of $AgNO_3$. The mixture was stirred at 80 °C for 1 h. The color of the solution turned from pale yellow into dark brown within 24 h, and indicated the reduction of silver ions into AgNPs [26].

Characterization of Green Synthesized Silver Nanoparticles (FA-AgNPs)

UV–Vis Spectroscopy

Ultraviolet–Visible (UV–Vis) spectroscopy is a well-established, simple and ideal tool for the characterization of metal nanoparticles that are specifically sensitive to concentration, size, shape and agglomeration state. In our study, the first step characterization of synthesized FA-AgNPs was assessed by the use of UV–Vis spectroscopy (PerkinElmer LS 40, USA), in a quartz cuvette. The reduction of silver ions to the nanoparticle form (AgNPs) was monitored by measuring the UV–Vis spectra of the solutions. The UV–Vis spectra of FA-AgNPs solution was recorded in an optical density range of 200 to 800 nm. Millipore water was used as the blank. Furthermore, with the aim to check the stability of the synthesized FA-AgNPs, same protocol was repeated for three times.

The formation of unique peak value at specific wavelength corresponds to the surface plasma resonance (SRP) of AgNPs. This peak value reflects the average size of the AgNP's size distribution. Moreover, no additional peaks reflect the successful purification of FA-AgNPs [26].

TEM

The shape, size and distribution of the synthesized FA-AgNPs was analyzed via TEM (JEOL JEM-1230 transmission electron microscope, Tokyo, Japan). It is a microscopic technique in which a beam of electrons is passed onto an ultrathin specimen. As a result, an image is formed from the interaction of a sample with the electron's beam which is further captured on an imaging device to check the shape, size and distribution of the synthesized nanoparticles.

The TEM observation was carried out by placing a drop of 8 µl of synthesized FA-AgNPs solution on a carbon coated copper grid (330 Mesh). It was then air dried and observed utilizing TEM at a 100 kV Accelerating Voltage [27].

Hydrodynamic Size, PDI and Zeta Potential

The hydrodynamic size, polydispersity index (PDI) and zeta potential of the green synthesized FA-AgNPs was measured through dynamic light scattering instrument (Zetasizer device, Malvern, Worcestershire, UK). It is a simple, easy and reliable tool for identifying particle size and surface charge. Nanoparticles were suspended in culture media and then sonicated via a sonicator bath (at room temperature for 15 min, at 40 W) to form homogenous mixture, and DLS measurement was performed.

The hydrodynamic size provides information about the mean nanoparticle size. The PDI is used to determine the degree of polydispersity in the sample. The zeta potential measurement is performed to evaluate the surface charge of the green synthesized nanoparticle which ultimately reflects their physical stability. A large positive or negative value of zeta potential of the nanoparticle gives clear indication for the good physical stability of nanoparticles [28].

FTIR

Fourier transform infrared (FTIR) spectrum measurement was used to determine the presence of possible functional groups of reducing agent (FA), involved in the synthesis of AgNPs. The FTIR spectrum bands were obtained for both aqueous extract (FA) and synthesized silver nanoparticles (FA-AgNPs), via utilizing FTIR spectroscopy (Nicolet 6700 FT-IR, Waltham, MA, USA). The sample analysis was performed in the most widely used spectrum region (the mid IR spectrum- '400–4000 cm^{-1}'). During analysis, samples are mixed with potassium bromide (KBR), and placed to contact with IR radiation which in turn have impacts on the atomic vibrations of a molecules in the sample, and thus reflect the specific absorption. The vibration of the molecules influenced by IR radiation at a particular wavelength is measured using FTIR. The analysis of FTIR is considered as a rapid, economical, and easy technique along with good accuracy [29].

Cell Culture, Exposure to FA Extract and FA-AgNPs, and MTT Assay

Human lung (A549) and cervical (HeLa) cancer cell lines were cultured in DMEM medium supplemented with 10% FBS, 100 U/ml penicillin, 50 µg/ml streptomycin and 1% Glutamine, at 5% CO_2 and 37 °C. At 85% confluence, cells were harvested utilizing 0.25% trypsin, and sub cultured into 96 well plates at the density of 2×10^5 cells/well in 100 µl optimized medium. Prior to treatment, cultured plates were incubated in CO_2 incubator and cells were allowed to attach the surface for 24 h. The medium was then aspirated and replaced with medium containing low to high doses (3.125, 6.25, 12.5, 25, 50 and 100 µl) of FA aqueous extract and synthesized FA-AgNPs, respectively. Treated cells were allowed to grow for further 48 h. At the end of incubation period, 100 µl of MTT reagent (filtered through a 0.22 µm filter) was added and kept in dark for 2 h. After the careful removal of medium containing MTT, 100 µl DMSO (Ajax Finechem Pty Ltd, Australia) was added to dissolve formazan crystals.

The 96-well-plate was also shaken for further 15 min in the dark to increase the dissolving of formazan crystals.

The absorbance of each treatment was measured at 490 nm using a 96-well plate reader (Molecular Devices -SPECTRA max- PLUS384). Each experiment was performed in three replicates, and untreated cells (controls) were run simultaneously. Absorbance values were normalized according to the controls. Hence, cell viability values of untreated cells should be 100%, while the cell viability of the treated cells should be below or above than 100%. The cell viability percentage was characterized as [Absorbance of treated cells/Absorbance of controls] × 100.

Molecular Analysis

Total RNA Extraction and cDNA Synthesis

A549 and HeLa cancer cells were cultured at a density of 2×10^2 cells/well in six well plates for 24 h, and exposed with FA aqueous extract and FA-AgNPs at low (6.25 µl) and high (25 µl) concentrations, respectively. Uuntreated cancer cells (controls) were also cultured simultaneously. After 48 h of incubation, total RNA was extracted from cultured cells using RNeasy Plus Mini kit (QIAGEN) according to the manufacturer's instructions. Concentration of the extracted RNA was measured via Nanodrop spectrophotometer (Thermo Scientific), and the quality of RNA were checked on agarose gel electrophoresis. The first strand cDNA was synthesized from 1.0 µg of total extracted RNA, utilizing cDNA Reverse Transcription Kit (Applied Biosystems), according to manufacturer's recommendations [30].

Gene Expression Analysis of Target Oncogenes by RT-qPCR

RT-qPCR of the target oncogenes (*PIK3CA*, *KRAS*, *EGFR* and *ERBB3*) was performed by Applied Biosystems SYBR Green PCR Master mix kit (Life Technologies, CA, USA), using StepOnePlus fluorescence quantitative PCR instrument (Applied Biosystems; Thermo Fisher Scientific, Inc., Waltham, MA, USA), following the manufacturer's instructions. GAPDH was used as an internal reference. Each sample was run in triplicate in a final volume of 12.5 µl containing 2 µl first-strand cDNA, 0.25 µl of each primer, 6.25 µl of SYBR Green PCR Master mix and 3.75 µl distilled water. The PCR conditions were as follows: initial denaturation at 95 °C for 10 min, followed by 40 cycles at 95 °C for 15 s, 60 °C for 60 s and elongation at 72 °C for 20 s [30]. The sequences of the specific sets of primers used for the genes *PIK3CA*, *KRAS*, *EGFR* and *ERBB3* are given in Table 1.

Statistical Analysis

Results are presented as Mean ± SD for at least three independent experiments. Statistical analyses were performed using SPSS software (version 25.0). Statistical differences between the groups were analysed through ANOVA and t-test. $p < 0.05$ was considered as significant.

Results

Characterization of Synthesized FA-AgNPs

The light yellow color *F. asafoetida* aqueous extract was used as a reducing agent in the green synthesis of AgNPs. When the colorless solution of $AgNo_3$ was mixed with the yellow aqueous extract of *F. asafoetida*, the color of the mixture turned into dark brown (within 24 h) and indicated the formation of synthesized FA-AgNPs (Fig. 1A).

The UV–Vis spectroscopy analysis reflects the strong absorption peak value at 432.5 nm, which corresponds to the surface Plasmon resonance of silver nanoparticles and confirms the formation of synthesized FA-AgNPs (Fig. 1B). The peak value for AgNPs is usually considered in the range 400–450 nm. In addition, it is cleared from Fig. 1B that UV–Vis spectra of FA-AgNPs showed no additional peaks which indicates the successful purification of FA-AgNPs.

Furthermore, the stability of FA-AgNPs was also checked through repeating the same protocol for three times. The color change pattern of the synthesized mixture was monitored and analysed utilizing UV–Vis spectroscopy. The stability of the synthesized FA-AgNPs was confirmed after recording the same absorption peak at 432.5 nm.

The morphology of the synthesized nanoparticles was determined through TEM and is shown in Fig. 2. The average TEM size of synthesized FA-AgNPs was in the range of 6–44 nm (average size- 20.64 nm), having good spherical shape structure and no significant agglomeration**.** The presence of TEM size range less than 100 nm clearly signifies the nano crystalline nature of FA-AgNPs which in turn

Table 1 List of the primers used for the RT-qPCR assay

Gene	Forward primers	Reverse primers
PIK3CA	5′-AGAGCCCCGAGCGTTTC-3′	5′-TCACCTGATGATGGTCGTGG-3′
KRAS	5′-TAGGCAAGAGTGCCTTGACG-3′	5′-CCCTCCCCAGTCCTCATGTA-3′
EGFR	5′-AAATGGGCTGCAAAGCTGTC-3′	5′-TTCCAGACAAGCCACTCACC-3′
ERBB3	5′-GAGGTGTGAGGTGGTGATGG-3′	5′-CGAATCCACTGCAGGAAGGA-3′

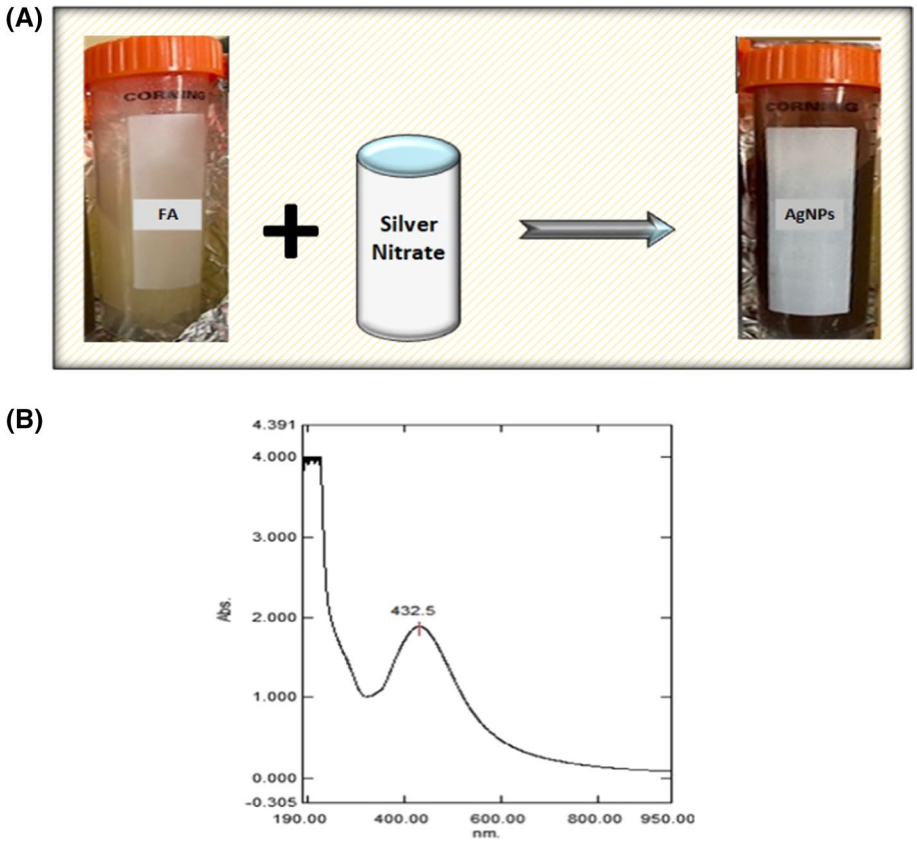

Fig. 1 **A** Green synthesis of silver nanoparticles (AgNPs) using *F. asafoetida* (FA) aqueous extract and 1 mM Silver nitrate aqueous solution. **B** The characterization of synthesized silver nanoparticles (FA-AgNPs) via UV–Vis spectroscopy

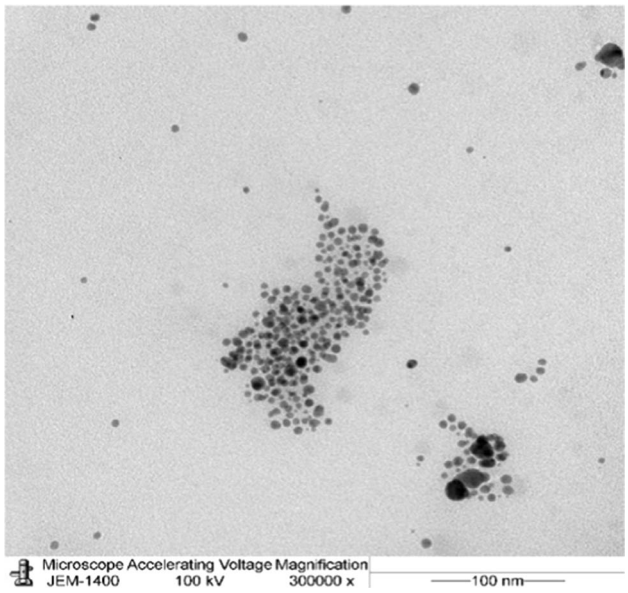

Fig. 2 The shape, size and distrbution of synthesized FA-AgNPs, utilizing TEM

promote its good catalytic and high accumulation property into the tumor area and support the further assessment of our study.

The hydrodynamic size of FA-AgNPs was 139.9 d.nm with a low PDI of 0.250, indicating the formation of monodispersed particles. The zeta potential value of FA-AgNPs as determined by DLS was − 0.684 mV, suggesting higher physical stability of silver nanoparticles (Fig. 3).

The FTIR spectra of FA and synthesized nanoparticles was analysed to confirm the presence of different functional groups of FA, involved in the capping, stabilization and reduction of synthesized AgNPs. The spectra were recorded in the wave range of 4000-400 cm^{-1} (Fig. 4A). The FTIR spectra of FA showed strong absorption peaks at 3427, 2926, 1656, 1159, 1021, 762, 575 cm^{-1} which represents various functional groups of FA. Moreover, the presence of more than five absorption peaks in the FTIR spectra of FA, clearly indicates its complex nature. Likewise, in a previous study, the complex property of FA was expressed via the presence of FTIR absorption peaks at 3405, 2427, 2359, 2100, 1788, 1635, 1338, 1048, and 832 cm^{-1} [31].

In our study, the strong absorption peak at 3427 cm^{-1} indicated the presence of O–H stretching of phenol/alcohol group. The presence of phenolic compound in the plant extract of FA has been already reported in many previous studies [32, 33]. Moreover, it is strongly postulated that the phenolic compound of FA might be involved in the reducing and capping of AgNPs. The absorption peak in the range of 2927 cm^{-1} was expressed as C–H stretching

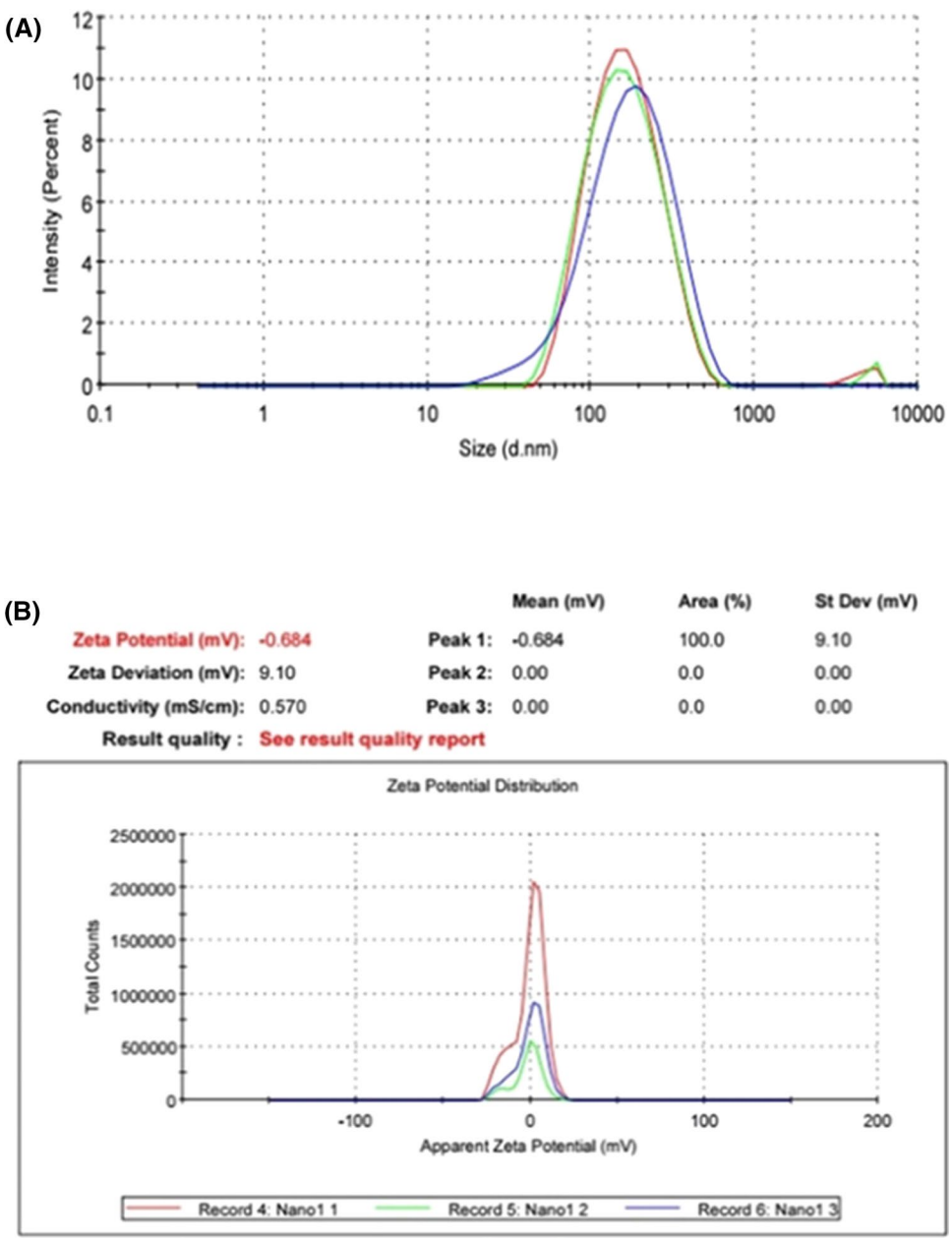

Fig. 3 The hydrodynamic size and zeta potential of synthesized FA-AgNPs, determined by DLS. **A** Hydrodynamic size of synthesized FA-AgNPs. **B** Zeta potential of synthesized FA-AgNPs

of the alkane group. In addition, the absorption band at 1656 cm^{-1} (−C=C− stretch) showed the features of alkenes group. The peak at 1159 cm^{-1} was expressed to $C=CH_2$ stretching and the peak near 762 and 575 cm^{-1} represented as −CH=CH− stretching of alkynes group. Manivasagan et al. study reveals that the groups of alcohols, phenolic, alkanes and alkynes have a strong capacity to interact with nanoparticles [34].

Similar to FA, the FTIR spectrum of synthesized FA-AgNPs showed strong absorption peaks at 3429, 2926, 1652, 1154, 1023, 763, and 575 cm^{-1} (Fig. 4A). Hence, the similarities in the peak values of the FTIR spectra of FA and synthesized FA-AgNPs along with some marginal shift clearly indicates the involvement of these different functional groups of FA in the binding of silver ions, respectively. Devanesan et al. also reported the FTIR absorption peaks at 3405, 2100, 1788, 1635, 1048, and 832 cm^{-1}, for the property of green synthesized AgNPs using FA [25]. The IR spectra of synthesized FA-AgNPs is also illustrated in Fig. 4B.

Hence, the conclusive results obtained from these various characterization methods, confirmed the successful synthesis of FA-AgNPs, which is clearly illustrated in Fig. 5.

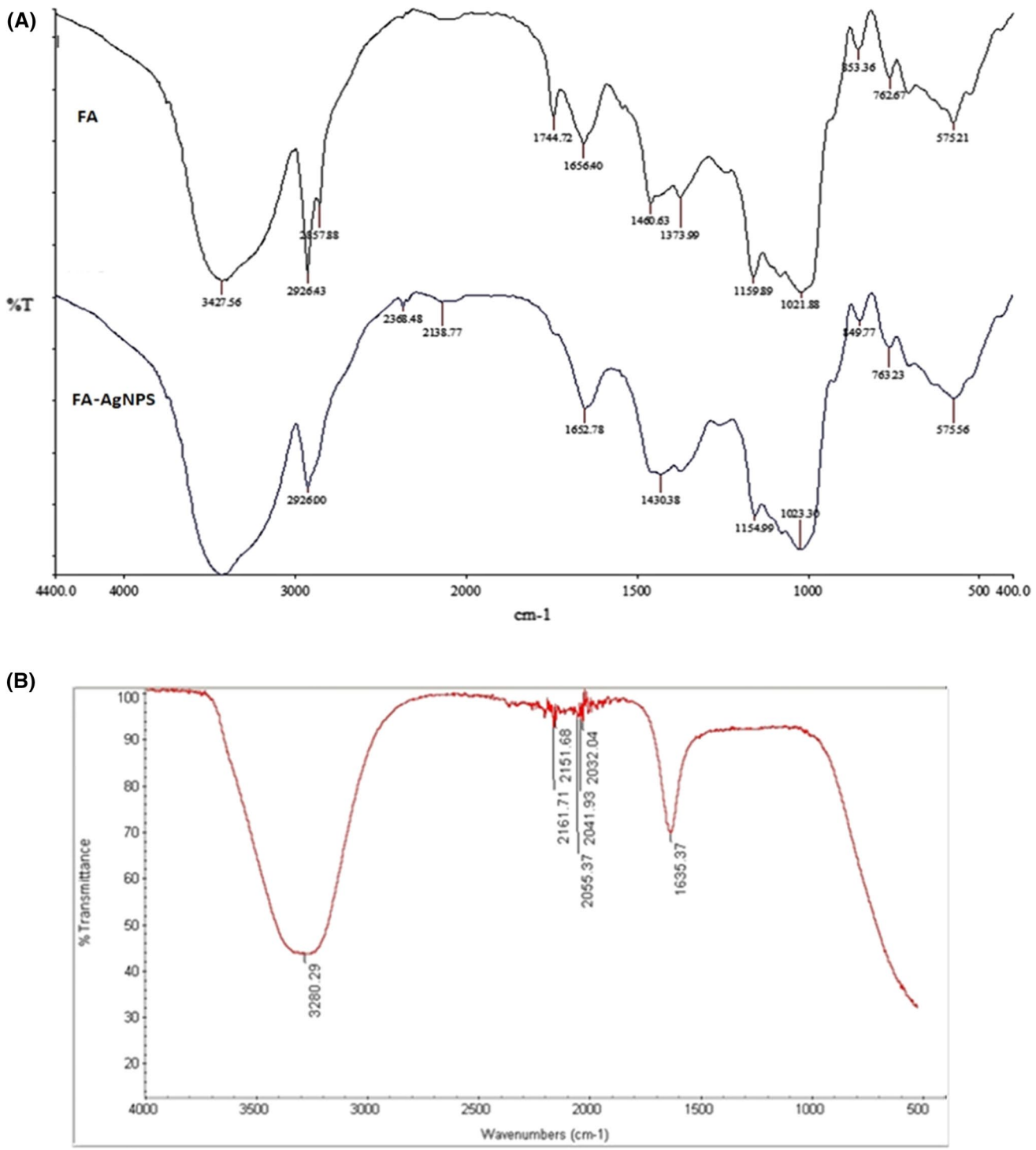

Fig. 4 **A** FTIR spectra of FA and synthesized FA-AgNPs, **B** IR spectra of synthesized FA-AgNPs

Cytotoxic Effects of FA Extract and Synthesized FA-AgNPs, in A549 and HeLa Cells

When A549 and HeLa cancer cells were treated with increasing doses (3.125, 6.25, 12.5, 25, 50 and 100 µl) of FA aqueous extract and synthesized FA-AgNPs for 48 h, the MTT assay showed that the viability of both studied cancer cells was considerably decreased in dose dependent manner (Fig. 6). Under different exposure conditions (3.125–100 µl) of FA aqueous extract, the percentage of cell viability of A549 cells was decreased to 95%, 82%, 79%, 55%, 47% and 24%. On the other hand, the cytotoxic effects of FA-AgNPs

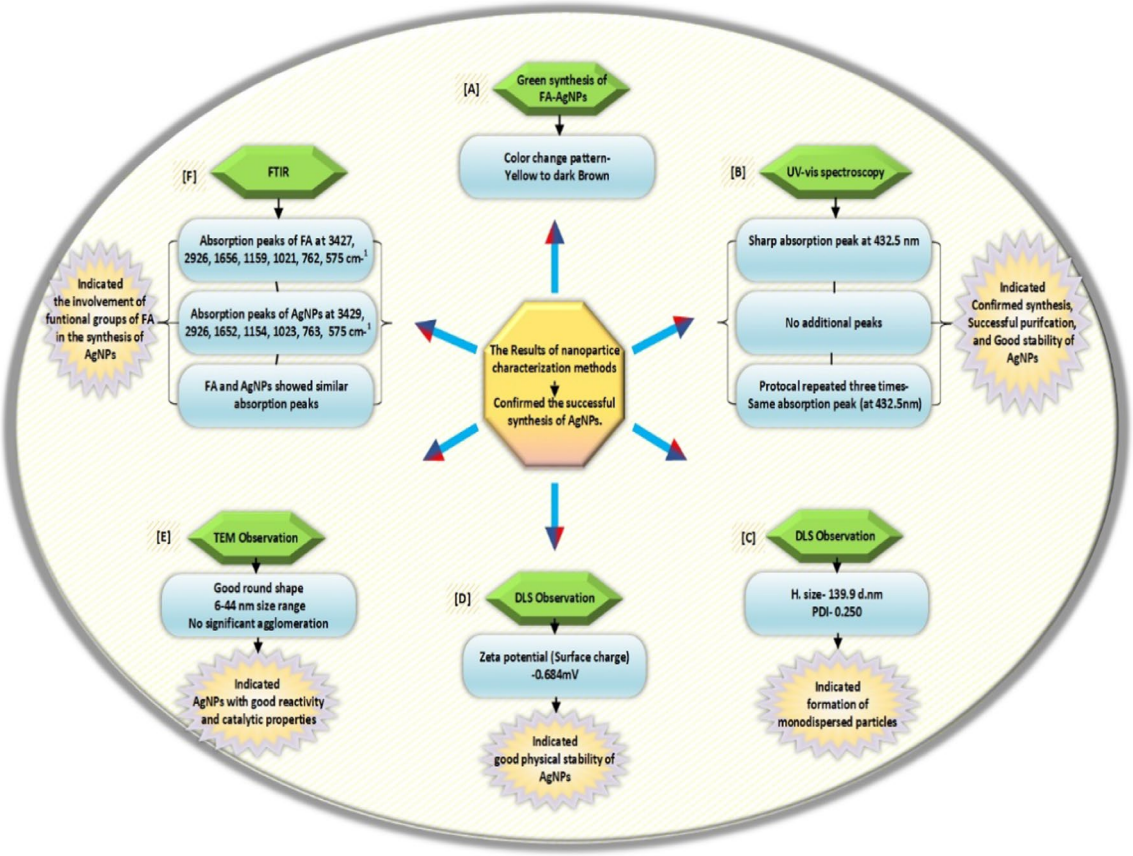

Fig. 5 Evidential illustration for the conclusive results of nanoparticles (FA-AgNPs) characterization methods which strongly proves that these methods are enough to demonstrate the successful synthesis of FA-AgNPs

in relation to A549 cells was exhibited in terms of higher rate of cell viability loss (90%, 27%, 26%, 22%, 20% and 11%) as compared to FA extract, at the same treatment doses (Fig. 6A).

Likewise, in case of HeLa cells, the cell viability was decreased to 99%, 96%, 78%, 73%, 66% and 10%, when cancer cells were treated with different increasing doses (3.125–100 µl) of FA extract. However, at the same treatment doses, FA-AgNPs induced cell viability reduction rate of HeLa cells was found to be higher (87%, 15%, 11%, 8%, 4% and 3%) as compared to the dose effects of FA extract (Fig. 6B).

The Average Low (6.25 µl) and High (25 µl) Doses of FA-AgNPs Causes Severe Cytotoxic Effects

Based on the conclusive findings of MTT assay, the doses of 6.25 µl and 25 µl were selected as an ideal and averagely low and high doses of FA-AgNPs to cause severe cytotoxic effects on both studied cancer cells, and further utilized for genetic analysis.

Under the low dose (6.25 µl) exposure effects of FA-AgNPs, the observed cell viability of A549 and HeLa cells was 27% and 15%, respectively. While the high dose (25 µl) effects of FA-AgNPs was indicated by the presence of 22% and 8% cell viability in A549 and HeLa cells, respectively (Fig. 6).

FA Extract and Synthesized FA-AgNPs Induced Genetic Effects

RT-qPCR was used to determine the expression levels of four oncogenes (*PIK3CA*, *KRAS*, *EGFR* and *ERBB3*) in treated A549 and HeLa cancer cells, under the low and high dose exposure effects of FA and FA-AgNPs. After 48 h of treatment period, RT-qPCR analysis showed that the expression of these four oncogenes was altered in studied cancer cells, due to the exposure effects of FA extract and FA-AgNPs (Figs. 7, 8, 9 and 10).

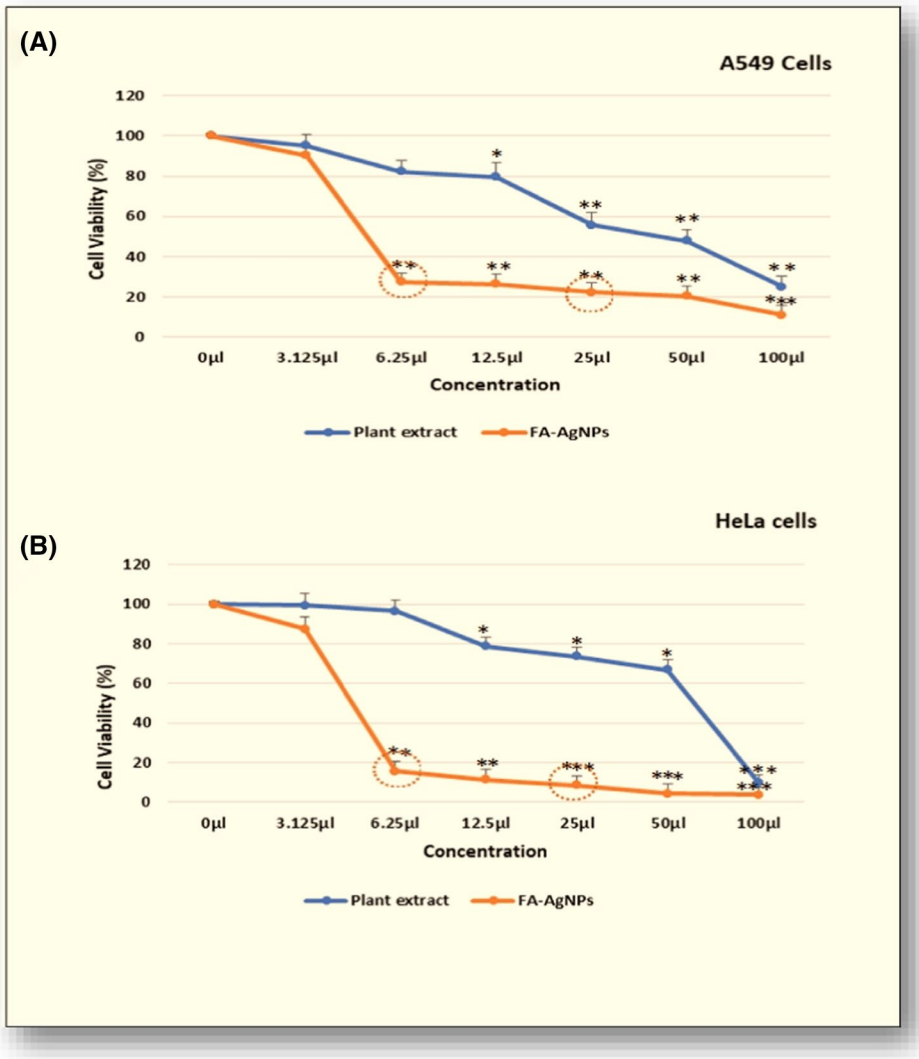

Fig. 6 The average low (6.25 µl) and high (25 µl) dose effects of FA-AgNPs causes strong cytotoxic effects on **A** A549 and **B** HeLa cancer cells. A549 and HeLa cells were treated with different increasing doses (3.125–100 µl) of FA And FA-AgNPs. Untreated cancer cells (0 µl) were used as controls. After 48 h, It was noted that FA-AgNPs induced cell viability loss was in higher rate compared to FA alone. The dose of 6.25 µl and 25 µl were observed as an averagely low and high doses of FA-AgNPs to cause strong cytotoxic effects against both studied cancer cells. Statistically significant difference as compared to controls indicates as ($p \leq 0.001$: ***, $p \leq 0.01$: **, $p \leq 0.05$: *)

Low and High Dose Effects of FA and FA-AgNPs on the Expression of Target Oncogenes, in A549 Cells

In case of treated A549 cells (Fig. 7), the low (6.25 µl) dose effects of FA extract and synthesized FA-AgNPs induces downregulation effects on the expression of *PIK3CA* and *KRAS* oncogenes as compared to controls. However, the downregulation effects of only FA-AgNPs was found to be significant ($p < 0.01$) in relation to the activity of these two oncogenes. In the further step, when the high dose (25 µl) effects of FA extract and FA-AgNPs were analysed towards the expression of four studied oncogenes (*PIK3CA*, *KRAS*, *EGFR* and *ERBB3*), in A549 cells (Fig. 8). The efficiency of FA extract and FA-AgNPs was capable to induce significant ($p < 0.05$) downregulation effects on the expression of *PIK3CA* and *KRAS* oncogenes in treated A549 cells than in controls. Moreover, we also noticed that FA-AgNPs induced downregulation effects for these two oncogenes, was more effective ($p < 0.01$) as compared to FA ($p < 0.05$) alone. On the other hand, the expression of the remaining two oncogenes *EGFR* and *ERBB3* was upregulated under the low and high dose effects of FA and FA-AgNPs in treated A549 cells, compared to controls (Figs. 7 and 8).

Low and High Dose Effects of FA and Synthesized FA-AgNPs on the Expression of Target Oncogenes, in HeLa Cells

In the next, when the low and high dose effects of FA extract and FA-AgNPs were analysed in favor of HeLa cancer cells. *PIK3CA* and *KRAS* were the two genes that were found to be downregulated in treated HeLa cells as compared to controls. However, the treatment efficiency of only FA-AgNPs was capable to induce significant ($p < 0.01$) downregulation effects on the expression of these two genes (*PIK3CA* and *KRAS*), at both low and high concentrations (Figs. 9 and 10).

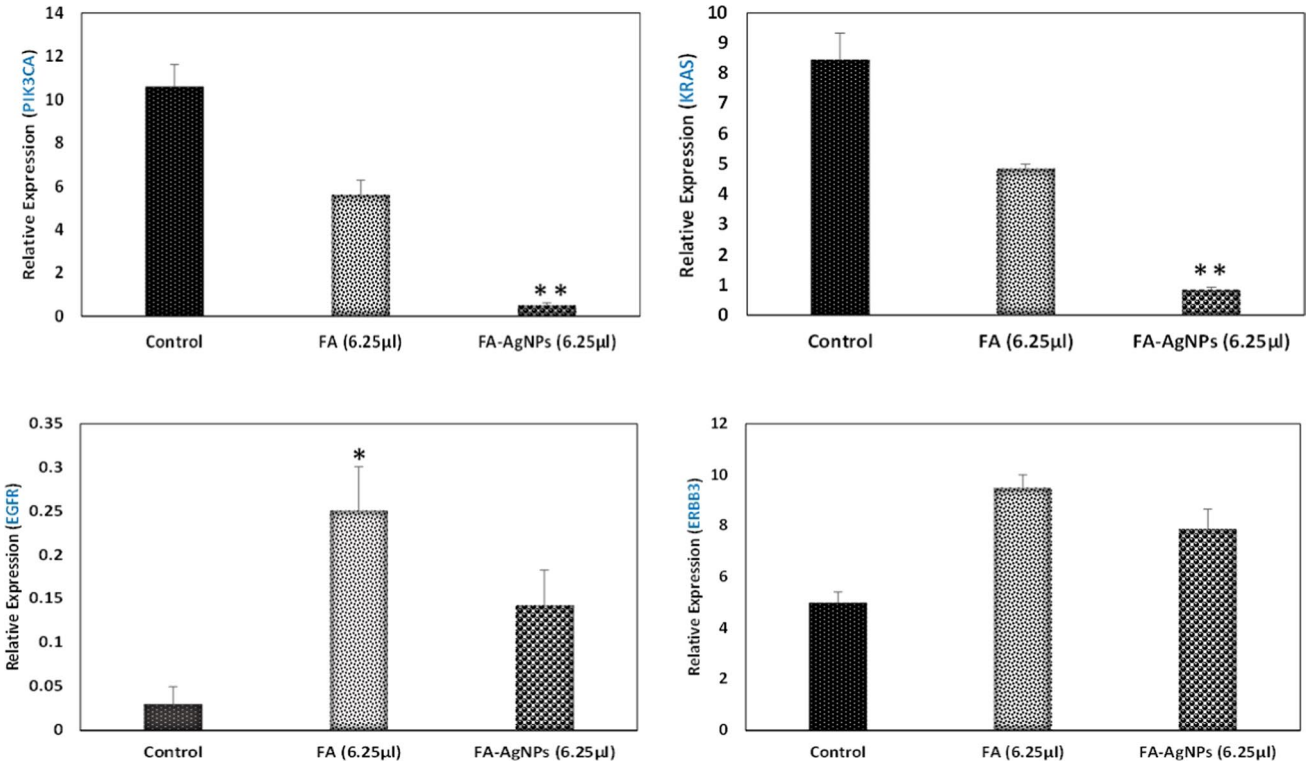

Fig. 7 The low dose (6.25 µl) effects of FA and synthesized FA-AgNPs on the expression of four oncogenes (*PIK3CA*, *KRAS*, *EGFR* and *ERBB3*), in A549 cells. A549 cells were treated with low dose (6.25 µl) of FA and synthesized FA-AgNPs. After 48 h of incubation, relative expression levels of these four oncogenes were analysed via RT-qPCR. Data are expressed as the mean values of three independent experiments. The results showed that the expression of *PIK3CA* and *KRAS* was downregulated in FA and FA-AgNPs treated A549 cells than in controls. However, only FA-AgNPs induced downregulation effects in relation to these two oncogenes was found to be significant (** $p < 0.01$) as compared to control. While the capability FA and FA-AgNPs was expressed to induce upregulation effects on the expression of the two remaining oncogenes (*EGFR* and *ERBB3*)

Similar to A549 cells, the low and high dose effects of FA and FA-AgNPs caused upregulation effects on the expression of *EGFR* and *ERBB3* oncogenes in treated HeLa cells as compared to controls (Figs. 9 and 10).

Discussion

The present study is the first-hand investigation showing the low dose (6.25 µl) capability of FA-AgNPs to induce strong cytotoxic action on lung and cervical cancer cells. Moreover, our study highlights molecular evidence of low dose mediated antitumor action of FA-AgNPs, which is related via its beneficial modulatory effects on the expression of *PIK3CA* and *KRAS* oncogenes, in lung and cervical cancer cells.

Lung cancer is one of the most fatal cancers that progress very rapidly with poor prognosis and short survival time. Due to limited treatment options, more than half of the patients diagnosed with lung cancer die within one year of diagnosis [35]. Likewise, cervical cancer is a serious disease that kills one woman in every two minutes [36]. Hence to date, the development of a potent and an effective therapy, is an urgent need to fight against these deadly diseases.

In recent years, the application of AgNPs in relation to its anticancer activity has achieved most popularity [6]. However, due to the involvement of hazardous chemicals, the high dose of chemically synthesized AgNPs causes various health complications on human body and in turn reduces the natural anticancer effectiveness of AgNPs [13, 37]. In this regard, plant-based green synthesis of AgNPs have been proved very effective in terms of having tremendous anticancer activities with quick results and lesser side effects [38]. Moreover, It is also postulated that the combination of plant extract and AgNPs can cause strong cytotoxicity with its low doses [39].

Despite intensive research on anticancer effects of green synthesized AgNPs, relatively very limited studies have been accomplished to determine the cytotoxic capability of FA based AgNPs, on different cancer cells [26, 31, 40]. Moreover, in all these previous studies, the researchers have mainly highlighted the high dose efficiency of FA-AgNPs to induce strong cytotoxic effects against various cancer cell lines.

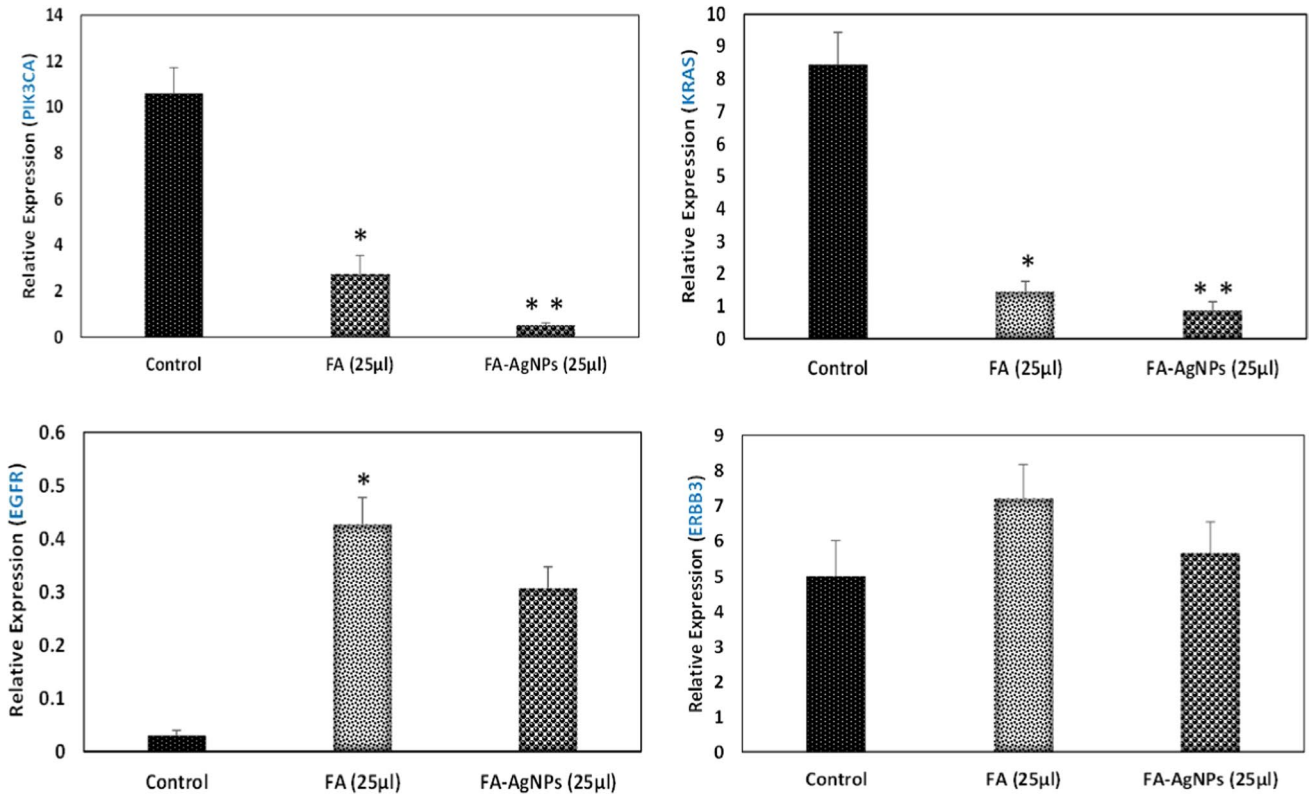

Fig. 8 The high dose (25 µl) effects of FA and synthesized FA-AgNPs on the expression of four oncogenes (*PIK3CA*, *KRAS*, *EGFR* and *ERBB3*), in A549 cells. When the relative expression levels of four oncogenes were checked under the exposure (at 25 µl dose for 48 h) effects of FA and FA-AgNPs, via RT-qPCR. PIK3CA and KRAS were the two oncogenes that were significantly downregulated in FA and FA-AgNPs treated A549 cells as compared to control. However, the downregulation effects of FA-AgNPs in relation to *PIK3CA* and *KRAS* was in greater extent (**$p < 0.01$) compared to FA (*$p < 0.05$). While the expression of *EGFR* and *ERBB3* was upregulated under the exposure condition of FA and FA-AgNPs

To the best of the author's knowledge, still now, there is no study that has particularly focussed on the low dose efficiency of FA-AgNPs against A549 and HeLa cells. Furthermore, the molecular evidence of low dose mediated anticancer action of FA-AgNPs is remain unclear.

Therefore, the present study initially focuses on the preparation of green synthesized AgNPs,

utilizing FA as a plant source, and for the first time checks the cytotoxic and molecular efficiency of FA and FA-AgNPs at low and high both doses, against A549 and Hela cancer cells.

In the first step, when the prepared FA mediated AgNPs were examined via color change pattern, UV–Vis spectroscopy, TEM, DLS, FTIR and IR. The results obtained from various assessment confirmed the formation of green synthesized FA-AgNPs having color change pattern of yellow to brown, strong UV–Vis absorption peak at 432.5 nm, size range of 6–44 nm, good spherical shape and no significant agglomeration. DLS observation with hydrodynamic size (139.9 d.nm) and low PDI indicated the formation of monodispersed particles. Zeta potential assessment also revealed the superior physical stability of AgNPs. The presence of various functional groups of FA on the surface of synthesized AgNPs was also confirmed by FTIR analysis (Fig. 5). It was an easy, economical and fast method along with no requirement of hazardous chemicals [26, 27, 29].

In the next, we utilized MTT assay and investigated the cytotoxic efficiency of FA extract and FA-AgNPs on A549 and Hela cancer cells. The results of the MTT assay revealed that different increasing doses (3.125, 6.25, 12.5, 25, 50 and 100 µl) of FA extract and FA-AgNPs (after 48 h) were capable to induce considerable cytotoxic effects on both treated cancer cells in dose dependent manner. Furthermore, we also observed that the cytotoxic potential of FA-AgNPs was in greater extent as compared to FA extract alone. Our results are consistent with many previous studies in which the efficiency of green synthesized AgNPs was proved to have significant cytotoxicity against cancer cells, in dose dependent manner [39, 40]. Likewise, pomegranate leaf extract, walnut green husk and cannonball leaf extract based green synthesis of AgNPs are found to have dose dependent effective cytotoxic effects against different cancer cell lines [29, 41, 42].

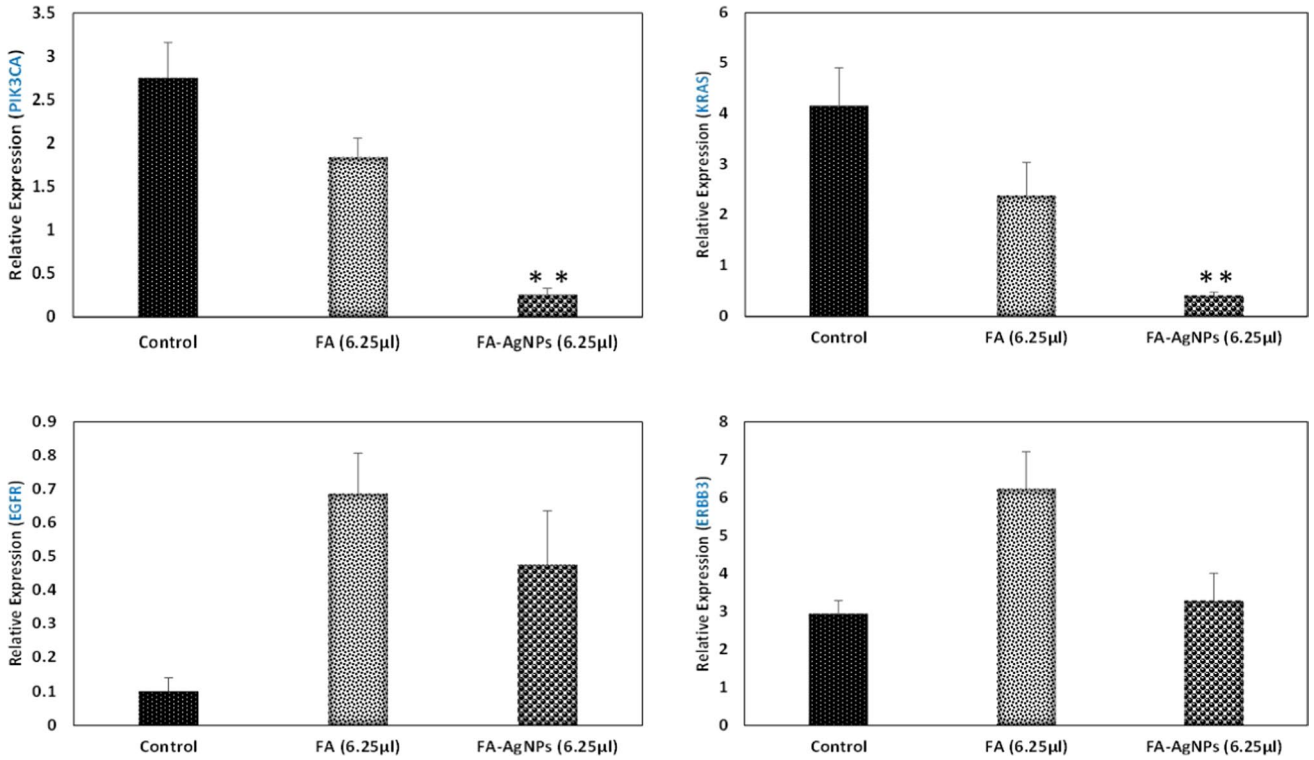

Fig. 9 The low dose (6.25 µl) effects of FA and synthesized FA-AgNPs on the expression of four oncogenes (*PIK3CA*, *KRAS*, *EGFR* and *ERBB3*), in HeLa cells. Under the low dose influence of FA and FA-AgNPs, the expression of *PIK3CA* and *KRAS* was downregulated in treated HeLa cells as compared to control. While *PIK3CA* and *KRAS* received significant (**$p<0.01$) downregulation effects only by the low dose effects of FA-AgNPs. Moreover, the low dose treatment of FA and FA-AgNPs showed no significant effects on the expression of the remaining two oncogenes (*EGFR* and *ERBB3*)

The superior cytotoxic efficiency of AgNPs is attributed due to increased formation of ROS. Hence, oxidative stress has been proposed as the main cytotoxic mechanism of AgNPs, In agreement with the study of Khorrami et al. [42], we postulate that due to large surface to volume ratio, the efficiency of AgNPs has the high tendency to enter into the exposed cells, and further interact with cellular constituents and in turn disturb the cellular signalling pathways. The interaction of AgNPs with cellular constituents leads increased formation of ROS causing progressive oxidative damage in terms of cell death [42]. Another study also reported that the mechanism of AgNPs induced toxicity may be linked with mitochondrial damage, DNA damage and oxidative stress [43].

On the other hand, the abnormal metabolism and high proliferation rate of cancerous cells encourage its uptake tendency towards AgNPs and eventually display enhanced AgNPs internalization, leading to a higher cell death rate [44].

Importantly, in our study, we found that the average low (6.25 µl) dose of FA-AgNPs was sufficient to induce strong cytotoxic effects against cancer cells, indicated by the presence of 27% and 15% cell viability on low dose treated A549 and HeLa cells, respectively. On the other hand, the average high (25 µl) dose effects of FA-AgNPs was expressed in the form of 22% and 8% cell viability on treated A549 and HeLa cells, respectively. Based on these collective findings, our study confirms the low dose efficiency of FA-AgNPs in terms of its strong anticarcinogenic role against lung and cervical cancer cells, and the extreme cytotoxicity induced by FA-AgNPs at lower concentration could be due to the plant component (FA) attached to the AgNPs [45].

FA is a good traditional medicine and widely recognised to treat various chronic and serious disorders [46]. One of the specific characteristics of this plant is its strong anticancer potential which is due to their antioxidant behaviour [18]. The rich constituents of FA including polyphenol, phenolic acid and flavonoid are found to have sufficient antioxidant potential and in turn exhibit inhibitory effects on tumor growth, angiogenesis and metastasis [47]. Among these constituents of FA, the role of polyphenol has been well studied against the progression of multiple cancers. In addition, the potential of polyphenol is reported to induce protective effects on healthy cells against free radical damage, and exerts toxic effects only for cancerous /unhealthy cells, which surely prompt the use of FA as a safe, natural

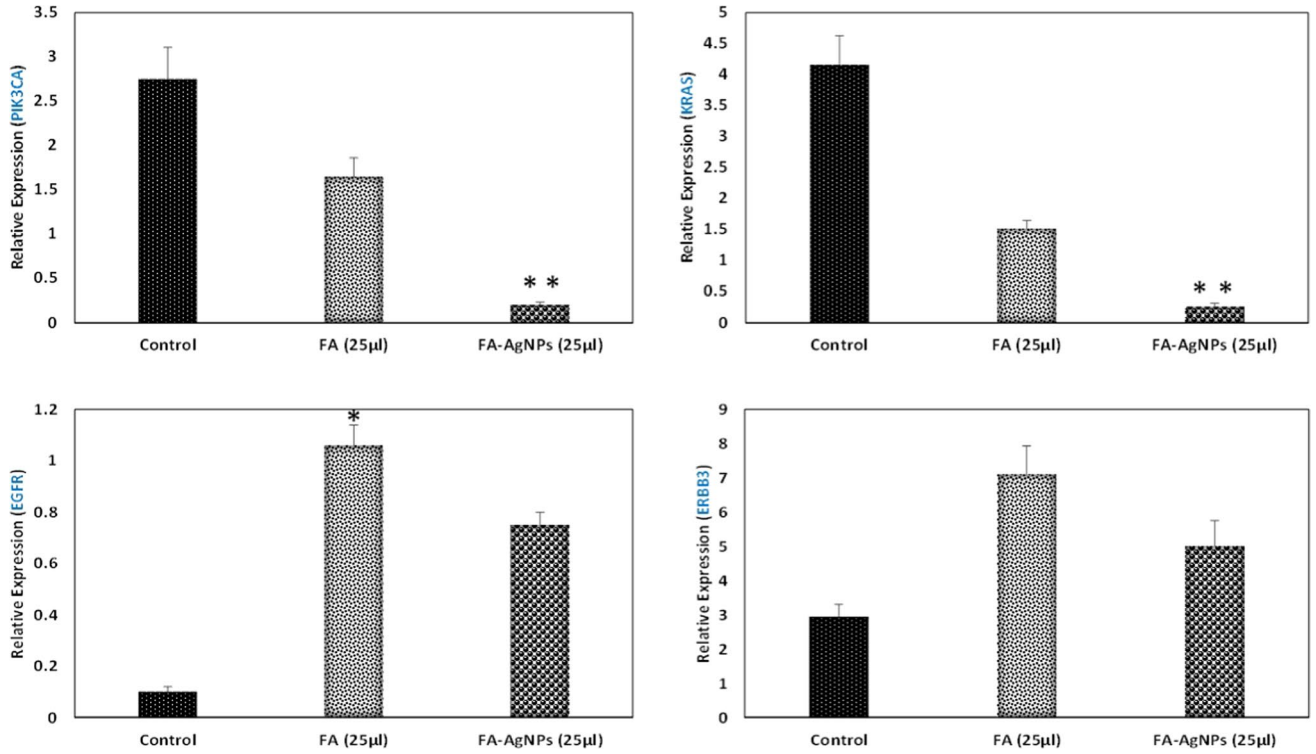

Fig. 10 The high dose (25 µl) effects of FA and Synthesized FA-AgNPs on the expression of four oncogenes (*PIK3CA*, *KRAS*, *EGFR* and *ERBB3*), in HeLa cells. The expression of two oncogenes (*PIK3CA* and *KRAS*) was significantly (**$p < 0.01$) reduced under the high dose exposure effects of FA-AgNPs. While the capability of FA was expressed to induce insignificant ($p > 0.05$) downregulation effects on the expression of these two oncogenes. Moreover, the high dose effects of FA and FA-AgNPs caused upregulation effects on the expression of the remaining two oncogenes (*EGFR* and *ERBB3*)

and efficient anti-tumor agent in cancer treatment [18, 19]. In line with these literatures, our study also concludes that the anticancer property of AgNPs can be safely maintained via the combination of a reliable agent FA.

Further, to explore the anti-tumor effects of FA extract and FA-AgNPs at molecular level, A549 and HeLa cancer cells were treated with low (6.25 µl) and high (25 µl) doses of FA extract and FA-AgNPs, respectively. After 48 h, RT-qPCR analysis showed that the expressions of four oncogenes (*PIK3CA*, *KRAS*, *EGFR* and *ERBB3*) were altered in treated cancer cells with slight (non-significant) and highly significant differences as compared to controls, which primarily indicates the capacity of FA extract and FA-AgNPs to induce modulations at genetic level in relation to these four oncogenes in target cancer cells.

It is well established that cancer is a multifactorial disease and the involvement of various genetic factors (such as PI3K/AKT, P53, NF-kB, STAT3 and COX-2 etc.) to prompt the initiation and progression of human cancer, has been studied in many previous studies [48, 49].

Among these factors, PI3K/AKT pathway has progressively received a major focus of interest as it plays an important role in regulating various cellular functions, including cell growth, metabolism, proliferation, survival, apoptosis, transcription and protein synthesis. Any mutation occurs in the genes that involved in the regulation of PI3K/AKT pathway, directly leads to the disturbance in normal cellular function, natural division and differentiation of cells, and in turn promote the development and progression of cancer cells [50]. According to the findings of many previous studies, the dysregulated activation (overactivation) of PI3K/AKT pathway has been recognised as one of the most important causes for the pathogenesis of lung and cervical cancers [51, 52]. In addition, multiple previous studies have emphasized the major involvement of four oncogenes (*PIK3CA*, *KRAS*, *EGFR* and *ERBB3*) in terms of its over expression leading to the overactivation of *PIK3CA* pathway. The overexpression of these four oncogenes together with the over activation of PI3K/AKT pathway represent a major molecular mechanism in the initiation and progression of cancer, which encourage researchers to develop novel treatment against lung and cervical cancers through targeting these four genes [22–24].

Hence, keeping in consideration about the major role of these four genes in the carcinogenesis of lung and cervical cancers, the present study also checks the low and high dose

effects of FA and FA-AgNPs on the expression of these target four oncogenes, in A549 and HeLa cancer cells.

In case of treated A549 cells, the low dose effects of FA and FA-AgNPs was expressed to induce beneficial modulations in terms of downregulation effects on the expression of *PIK3CA* and *KRAS* oncogenes, compared to controls. However, the capacity of only FA-AgNPs was noted in the form of its highly significant downregulation effects in relation to both oncogenes in treated A549 cells compared to controls. While under the high dose exposure condition of FA and FA-AgNPs, the expression of both oncogenes (*PIK3CA* and *KRAS*) was significantly decreased in treated A549 cells than in controls. But, the modulating tendency of FA-AgNPs to decrease the activity of *PIK3CA* and *KRAS* was more effective as compared to FA exposure effects.

Likewise, in case of Hela cells, *PIK3CA* and *KRAS* were two genes that were observed in downregulated stages under the low and high dose exposure condition of FA and FA-AgNPs. However, these two oncogenes received significant downregulation effects in response to only low and high dose exposure condition of FA-AgNPs. Based on these results, we postulated that the low dose of FA-AgNPs was sufficient to cause strong downregulation effects on the expression of *PIK3CA* and *KRAS* oncogenes in treated both cancer cells than in control. While the capability of FA-AgNPs was not expressed to show downregulation effects on the expression of the remaining two oncogenes (*EGFR* and *ERBB3*), in studied A549 and HeLa cancer cells.

PIK3CA gene is one of the most commonly mutated oncogenes, present in human cancer. Many previous studies have confirmed the presence of over expressed *PIK3CA* gene in high frequency in the carcinogenesis of lung and cervical cancer cells [22, 53]. Likewise, the role of *KRAS* gene has been found in its overexpressed stage to exhibit a major contribution in the initiation and progression of lung and cervical cancers [54, 55]. Hence, in agreement to these previous studies, the results of our study clearly signify the strong anticarcinogenic modulatory effects of FA-AgNPs at relatively low concentration which is associated with significantly decreased expression of *PIKCA* and *KRAS* oncogenes in treated lung and cervical cancer cells.

Conclusion

In conclusion, the present study has successfully synthesized silver nanoparticles (FA-AgNPs) utilizing a natural and safer anti-tumor agent *Ferula asafoetida*. It was a cost-effective method with no requirement of hazardous chemicals. The low dose of synthesized FA-AgNPs was found to be sufficient to induce strong cytotoxic effects on the growth of lung and cervical cancer cells. Importantly, our study provides new information for the molecular evidence of strong anticancer effects of synthesized FA-AgNPs which is mediated via it's lose dose effects to significantly decrease the expression of two crucial cancer promoting genes (*PIK3CA* and *KRAS*) in treated lung and cervical cancer cells. Overall, the findings of our study conclude that the combination of low dose of AgNPs and *Ferula asafoetida* can offer robust anticancer effects without any adverse effects.

Acknowledgements This present research was supported by a grant from the Research Centre of the Female Scientific and Medical Colleges, King Saud University, Riyadh, Saudi Arabia. The authors express thank the Deanship of Scientific Research and RSSU at King Saud University for their technical support. The authors are also grateful for the support of Manal A. Awad (King Abdullah Institute for Nanotechnology, King Saud University), in nanoparticle preparation.

Funding The present study was funded by a grant from the Research Centre of the Female Scientific and Medical Colleges, King Saud University, Riyadh, Saudi Arabia.

Data Availability The datasets used and/or analysed during the current study are available from the corresponding author on reasonable request.

Declarations

Conflict of interest The authors declare that they have no known competing financial interests or personal relationships that could have appeared to influence the work reported in this paper.

References

1. H. Sung, J. Ferlay, and L. Rebecca (2016). *CA Cancer J. Clin.* **71**, 209.
2. J. Zhang, J. Li, S. Xiong, et al. (2021). *Ann Cancer Epidemiol.* **5**, 4.
3. W. Q. He and C. Li (2021). *Gynecol. Oncol.* **163** (3), 583.
4. A. L. Couffignal, M. Lapeyre-Mestre, C. Bonhomme, et al. (2000). *Therapie* **55** (5), 635.
5. C. Jin, K. Wang, A. Oppong-Gyebi, et al. (2020). *Int. J. Med. Sci.* **17** (18), 2964.
6. H. I. O. Gomes, C. S. M. Martins, and J. A. V. Prior (2021). *Nanomaterials* **11**, 964.
7. N. E. A. El-Naggar, M. H. Hussein, and A. A. El-Sawah (2017). *Sci. Rep.* **7** (1), 20.
8. S. Barua, P. P. Banerjee, A. Sadhu, et al. (2017). *J. Nanosci. Nanotechnol.* **7** (2), 968.
9. F. M. Gutierrez, E. P. Thi, J. M. Silverman, et al. (2012). *Nanomed.: Nanotechnol. Biol. Med.* **8** (3), 328.
10. X. F. Zhang, Z. G. Liu, and W. Shen (2016). *Int. J. Mol. Sci.* **17**, 1534.
11. M. Korani, E. Ghazizadeh, S. Korani, Z. Hami, and A. Mohammadi-Bardbori (2016). *Eur. J. Nanomed.* **7** (1), 51.
12. B. Mao, Z. Y. Chen, Y. J. Wang, and S. J. Yan (2018). *Sci. Rep.* **8** (1), 2445.
13. S. Kummara, M. B. Patil, and T. Uriah (2016). *Biomed. Pharmacother.* **84**, 10.
14. S. Jabeen, S. Qureshi, and M. Munazir (2021). *Mater. Res. Express* **8** (9), 092001.
15. A. Amalraj and S. Gopi (2017). *J. Tradit. Complement. Med.* **7**, 347–359.

16. R. Panwar, S. Rana, and D. K. Dhawan (2015). *J. Phytopharm.* **4**, 282.
17. M. Abroudi, A. G. Fard, and G. Dadashizadeh (2020). *Int. J. Biomed. Eng. Clin. Sci.* **6** (3), 60.
18. S. M. Bagheri, A. A. Asl, and M. T. Moghadam (2017). *J. Ayurveda Integr. Med.* **8** (3), 152.
19. A. A. Dehpour, M. A. Ebrahimzadeh, N. S. Fazel, et al. (2009). *Grasas y Aceites.* **60**, 405.
20. Iksen, S. Pothongsrisit, V. Pongrakhananon (2021). Molecules **26**, 4100.
21. J. K. Schwarz, J. E. Payton, and R. Rashmi (2012). *Clin Cancer Res.* **18** (5), 1464.
22. H. Yamamoto, H. Shigematsu, and M. Nomura (2008). *Cancer Res.* **68** (17), 6913.
23. V. Jurisic, J. Obradovi, and S. Pavlovic (2016). *OncoTargets Therapy* **9**, 6065.
24. B. Duan, Z. Zhu, B. You, et al. (2019). *Int. J. Clin. Exp. Pathol.* **12** (8), 2931.
25. S. Devanesan, K. Ponmurugan, M. S. AlSalhi, et al. (2020). *Int. J. Nanomed.* **15**, 4351.
26. A. E. Mohammed, A. Al-Qahtani, A. Al-Mutairi, et al. (2018). *Nanomaterials* **8**, 382.
27. A. Bandyopadhyay, B. Roy, P. Shaw, et al. (2020). *Nucleus* **63**, 191–202.
28. S. Mukherjee, D. Chowdhury, and R. Kotcherlakota (2014). *Theranostics* **4**, 316.
29. P. Devaraj, P. Kumari, C. Aarti, et al. (2013). *J Nanotechnol*. https://doi.org/10.1155/2013/598328.
30. M. Ahmad, H. A. Alhadlaqb, J. Ahmad, et al. (2015). *J. Appl. Toxicol.* **35**, 640.
31. S. N. Abootalebi, S. M. Mousavi, and S. A. Hashemi (2021). *Hindawi J Nanomater*. https://doi.org/10.1155/2021/6676555.
32. H. Ahmadvand, H. Amiri, Z. D. Elmi et al. (2013). Iran. J. Pharmacol. Therap. **12** (2), 52.
33. R. Niazmand and B. M. Razavizadeh (2021). *J. Food Sci. Technol.* **58** (6), 2148.
34. P. Manivasagan, J. Venkatesan, K. Senthilkumar, et al. (2013). *BioMed Res Int*. https://doi.org/10.1155/2013/287638.
35. X. Wu, J. Li, and W. Du (2022). *BMC Pulm. Med.* **22**, 1–17.
36. D. K. Gaffney, M. Hashibe, D. Kepka, et al. (2018). *Gynecol. Oncol.* **151** (3), 547.
37. W. Younas, F. U. Khan, M. Zaman, et al. (2022). *Sci. Total Environ.* **845**, 157366.
38. C. Hano and B. H. Abbasi (2022). *Biomolecules* **12**, 31.
39. P. Palaniappan, G. Sathishkumar, and R. Sankar (2015). *Spectrochim. Acta A Mol. Biomol. Spectrosc.* **138**, 885.
40. N. C. Than, A. C. Chinnathambi, T. A. Alahmadi, et al. (2022). *J Nanomater*. https://doi.org/10.1155/2022/6095005.
41. S. Devanesan, M. S. AlSalhi, and R. V. Balaji (2018). *Nanoscale Res. Lett.* **13**, 315.
42. S. Khorrami, A. Zarrabi, M. Khaleghi, et al. (2018). *Int. J. Nanomed.* **13**, 8013.
43. L. Xin, J. Wang, and G. Fan (2015). *Environ. Toxicol.* **31** (12), 1691.
44. R. A. Cairns, I. S. Harris, and T. W. Mak (2011). *Nat. Rev Cancer* **11** (2), 85.
45. M. A. Farah, M. A. Ali, S. M. Chen, et al. (2016). *Colloid Surf. B* **141**, 158.
46. A. Amalraj and S. Gopi (2017). *J. Tradit. Complement. Med.* **7** (3), 347.
47. H. Ahmadvand, H. Amiri, Z. D. Elmi, et al. (2013). *Iran. J. Pharmacol. Therap.* **12** (2), 52.
48. N. Jiang, Q. Dai, X. Su, et al. (2020). *Mol. Biol. Rep.* **47**, 4587.
49. M. M. Chaturvedi, B. Sung, and V. R. Yadav (2011). *Oncogene* **30**, 1615.
50. F. Chang, J. T. Lee, and P. M. Navolanic (2003). *Leukemia* **17**, 590.
51. E. G. Sarris, M. W. Saif, and K. N. Syrigos (2012). *Pharmaceuticals* **5** (11), 1236.
52. S. Stavros, K. Pappa, and P. Drakakis (2019). *HJOG* **18** (4), 111.
53. A. A. Wright, B. E. Howitt, A. P. Myers, et al. (2013). *Cancer* **119** (21), 3776.
54. N. Sunaga, K. Kaira, H. Imai, et al. (2013). *Oncogene* **32** (34), 4034.
55. L. Huang, Z. Guo, F. Wang, et al (2021) Signal. Transduct. Target. Ther **6** (386), 20.